How sensitive are various NN observables to changes in the πNN coupling constant? *

R. Machleidt
Department of Physics, University of Idaho,
Moscow, Idaho 83844, U. S. A.

September 17, 1999

Abstract

The deuteron, NN analyzing powers A_y, and the singlet scattering length show great sensitivity to the πNN coupling constant g_π. While the pp A_y data favor $g_\pi^2/4\pi \leq 13.6$, the np A_y data and the deuteron quadrupole moment imply $g_\pi^2/4\pi \geq 14.0$. The two diverging values could be reconciled by the assumption of (substantial) charge-splitting of g_π. However, the established theoretical explanation of the charge-dependence of the $^1S_0$ scattering length (based upon pion mass splitting) is very sensitive to a difference between g_{π^0} and $g_{\pi^\pm}$ and rules out any substantial charge-splitting of g_π. Thus, there are real and large discrepancies between the values for g_π extracted from different NN observables. Future work that could resolve the problems is suggested.

*Invited talk presented at the Workshop on *Critical Points in the Determination of the Pion-Nucleon Coupling Constant*, Uppsala (Sweden), June 7-8, 1999.

1 Introduction

In this contribution, I will focus on the deuteron, NN analyzing powers, and the singlet scattering length. Other NN observables with sensitivity to the πNN coupling constant are the spin transfer coefficients $D_{NN'}$, $D_{LL'}$, and $D_{SS'}$ which are discussed in the contribution by Scott Wissink and in Ref, [1].

2 The deuteron

In the 1980's, Torleif Ericson pointed out repeatedly [2] that the deuteron is the most convincing manifestation of the 'existence' of the pion in nuclear physics. Historically, it was the non-vanishing quadrupole moment of the deuteron that provided the first evidence for a nuclear tensor force, which is created by the pion. Also, while the theoretical explanation of NN scattering observable requires, in general, to take several mesons into account, the deuteron can be described by the pion alone (together with a semi-soft πNN form factor). Thus, there are good physics reasons why the deuteron should show a great deal of sensitivity to the πNN coupling constant, g_π.

The crucial deuteron properties to consider are the quadrupole moment, Q, and the asymptotic D/S state ratio, η. The sensitivity of both quantities to g_π is demonstrated in Table I. The calculations are based upon the most recent Bonn potential ('CD-Bonn' [3]) which belongs to the new generation of high-precision NN potentials that fit the NN data below 350 MeV with a 'perfect' χ^2/datum of about one. The numbers in Table I are an update of earlier calculations of this kind [4, 5] in which older NN potentials were applied. There are no substantial differences in the results as compared to the earlier investigations.

For meaningful predictions, it is important that all deuteron models considered are realistic. This requires that besides the deuteron binding energy (that is accurately reproduced by all models of Table I) also other empirically well-known quantities are correctly predicted, like the deuteron radius, r_d, and the triplet effective range parameters, a_t and r_t. As it turns out, the latter quantities are closely related to the asymptotic S-state of the deuteron, A_S, which itself is not an observable. However, it has been shown [2] that for realistic values of r_d, a_t, and r_t, the asymptotic S-state of the deuteron comes out to be in the range $A_S = 0.8845 \pm 0.0008$ fm$^{-1/2}$. Thus, A_S plays

Table I. Important coupling constants and the predictions for the deuteron and some *pp* phase shifts for five models discussed in the text.

	A	B	C	D	E	Empirical
Important coupling constants						
$g^2_{\pi^0}/4\pi$	13.6	13.6	14.0	14.4	13.6	
$g^2_{\pi^\pm}/4\pi$	13.6	13.6	14.0	14.4	14.4	
κ_ρ	6.1	3.7	6.1	6.1	6.1	
The deuteron						
Q (fm^2)	0.270	0.278	0.276	0.282	0.278	0.276(2)[a]
η	0.0255	0.0261	0.0262	0.0268	0.0264	0.0256(4)[b]
A_S (fm$^{-1/2}$)	0.8845	0.8842	0.8845	0.8845	0.8847	0.8845(8)[c]
P_D (%)	4.83	5.60	5.11	5.38	5.20	–
$^3P_0$ *pp* phase shifts (deg)						
10 MeV	3.726	4.050	3.881	4.039	3.726	3.729(17)[d]
25 MeV	8.588	9.774	8.981	9.384	8.588	8.575(53)[d]
50 MeV	11.564	14.070	12.158	12.763	11.564	11.47(9)[d]

[a]) Corrected for meson-exchange currents and relativity [6].
[b]) Ref. [9].
[c]) Ref. [2].
[d]) Nijmegen *pp* multi-energy phase shift analysis [10].

the role of an important control number that tells us if a deuteron model is realistic or not. As can be seen from Table I, all our models pass the test.

Model A of Table I uses the currently fashionable value for the πNN coupling constant $g^2_\pi/4\pi = 13.6$ which clearly underpredicts Q while η is fine. One could now try to fix the problem with Q by using a weaker ρ-meson tensor-coupling to the nucleon, f_ρ. It is customary to state the strength of this coupling in terms of the tensor-to-vector ratio of the ρ coupling constants, $\kappa_\rho \equiv f_\rho/g_\rho$. Model A uses the 'large' value $\kappa_\rho = 6.1$ recommended by Hoehler and Pietarinen [11]. Alternatively, one may try the value implied by the vector-meson dominance model for the electromagnetic form factor of the nucleon [12] which is $\kappa_\rho = 3.7$. This is done in our Model B which shows the desired improvement of Q. However, a realistic model for the NN interaction must not only describe the deuteron but also NN scattering. As discussed in detail in Ref. [13], the small κ_ρ cannot reproduce the ϵ_1 mixing parameter correctly and, in addition, there are serious problems with the ^3P_J phase shifts, particularly, the $^3P_0$ (cf. lower part of Table I and Fig. 1). Therefore, Model B is unrealistic and must be discarded.

The only parameters left to improve Q are g_π and the cutoff mass, Λ_π, that is used to parametrize the πNN form factor (cf. Eq. (6) below). Similar, to the ρ meson, Λ_π is heavily constrained by NN phase parameters, particularly, ϵ_1. The accurate reproduction of ϵ_1 as determined in the Nijmegen np multi-energy phase shift analysis [10] essentially leaves no room for variations of Λ_π once the ρ meson parameters are fixed.

Thus, we are finally left with only one parameter to fix the Q problem, namely g_π. As it turns out, for relatively small changes of $g_\pi^2/4\pi$ there is a linear relationship, as demonstrated in Table I by the predictions of Model A, C and D which use $g_\pi^2/4\pi = 13.6$, 14.0, and 14.4, respectively. Consistent with our earlier studies [4, 5], we find that $g_\pi^2/4\pi \geq 14.0$ is needed to correctly reproduce Q.

However, a pion coupling with $g_\pi^2/4\pi \geq 14.0$ creates problems for the $^3P_0$ phase shifts which are predicted too large at low energy (cf. lower part of Table I and Fig. 1). Now, a one-boson-exchange (OBE) model for the NN interaction includes several parameters (about one dozen in total). One may therefore try to improve the $^3P_0$ by readjusting some of the other model parameters. The vector mesons (ρ and ω) have a strong impact on the $^3P_0$ (and the other P waves). However, due to their heavy masses, they are more effective at high energies than at low ones. Therefore, ρ and ω may produce large changes of the $^3P_0$ phase shifts in the range 200-300 MeV, with little improvement at low energies. The bottom line is that in spite of the large number of parameters in the model, there is no way to fix the $^3P_0$ at low energies. In this particular partial wave, the pion coupling constant is the only effective parameter, at energies below 100 MeV. The pp phase shifts of the Nijmegen analysis [10] as well as the pp phases produced by the VPI group [14] require $g_\pi^2/4\pi \leq 13.6$.

Notice that this finding is in clear contradiction to our conclusion from the deuteron Q.

There appears to be a way to resolve this problem. One may assume that the neutral pion, π^0, couples to the nucleon with a slightly different strength than the charged pions, $\pi^\pm$. This assumption of a charge-splitting of the πNN coupling constant is made in our Model E where we use $g_{\pi^0}^2/4\pi = 13.6$ and $g_{\pi^\pm}^2/4\pi = 14.4$. This combination reproduces the pp $^3P_0$ phase shifts at low energy well [15] and creates a sufficiently large deuteron Q.

Table II. χ^2/datum for the fit of the world *pp* A_y data below 350 MeV (subdivided into three energy ranges) using different values of the πNN coupling constant [15].

	Coupling constant $g^2_{\pi^0}/4\pi$			
Energy range (# of data)	13.2	13.6	14.0	14.4
		A	C	D
0–17 MeV (45 data)	0.84	1.43	2.71	4.66
17–125 MeV (148 data)	1.05	1.06	1.54	2.45
125–350 MeV (624 data)	1.24	1.22	1.26	1.34

3 Analyzing powers

In our above considerations, some *pp* phase shifts played an important role. In principle, phase shifts are nothing else but an alternative representation of data. Thus, one may as well use the data directly. Since the days of Gammel and Thaler [16], it is well-known that the triplet P-wave phase shifts (which we focused on, above) are fixed essentially by the NN analyzing powers, A_y. Therefore, we will now take a look at A_y data and compare them directly with model predictions.

In Fig. 2, we show high-precision *pp* A_y data at 9.85 MeV from Wisconsin [17]. The theoretical curves shown are obtained with $g^2_{\pi^0}/4\pi = 13.2$ (dotted), 13.6 (solid), and 14.4 (dash-dot) and fit the data with a χ^2/datum of 0.98, 2.02, and 9.05, respectively. Clearly, a small coupling constant around 13.2 is favored. Since a single data set is not a firm basis, we have looked into all *pp* A_y data in the energy range 0–350 MeV. Our results are presented in Table II where we give the χ^2/datum for the fit of the world *pp* A_y data below 350 MeV (subdivided into three energy ranges) for various choices of the neutral πNN coupling constant. It is seen that the *pp* A_y data at low energy, particularly in the energy range 0–17 MeV, are very sensitive to the πNN coupling constant. A value $g^2_{\pi^0}/4\pi \leq 13.6$ is clearly preferred, consistent with what we extracted from the single data set at 9.85 MeV as well as from $^3P_0$ phase shifts in the previous section (cf. Fig. 1).

Next, we look into the *np* A_y data. A single sample is shown in Fig. 3, the *np* A_y data at 12 MeV from TUNL [18]. Predictions are shown for Model A (solid line), D (dash-dot), and E (dash-triple-dot). The charge-splitting

Table III. χ^2/datum for the fit of various sets of np A_y data using different values for the πNN coupling constants.

	Coupling constants $g^2_{\pi^0}/4\pi$; $g^2_{\pi^\pm}/4\pi$				
Energy, data set (# of data)	13.6; 13.6	14.0; 14.0	14.4; 14.4	13.6; 14.0	13.6; 14.4
	A	C	D		E
12 MeV [18] (9 data)	2.81	2.27	1.79	1.53	1.00
7.6–18.5 MeV [18] (31 data)	1.89	1.56	1.29	1.28	1.32
0–17 MeV world data (120)	1.17	1.03	0.94	0.99	1.19
17–50 MeV [19] (85 data)	1.16	1.12	1.14	1.18	1.18
17–125 MeV world data (416)	0.89	0.89	0.91	0.91	0.94

Model E fits the data best with a χ^2/datum of 1.00 (cf. Table III). We have also considered the entire np A_y data measured by the TUNL group [18] in the energy range 7.6–18.5 MeV (31 data) as well as the world np A_y data in the energy ranges 0–17 MeV (120 data). It is seen that there is some sensitivity to the πNN coupling constant in this energy range, while there is little sensitivity at energies above 17 MeV (cf. Table III).

Consistent with the trend seen in the 12 MeV data, the larger data sets below 17 MeV show a clear preference for a coupling constant around 14.4 if there is no charge splitting of g_π. This implies that without charge-splitting it is impossible to obtain an optimal fit of the pp and np A_y data. To achieve this best fit charge-splitting is needed, like $g^2_{\pi^0}/4\pi = 13.6$ and $g^2_{\pi^\pm}/4\pi = 14.0$ as considered in column 5 of Table III. The drastic charge-splitting of Model E is not favored by the more comprehensive np A_y data sets.

The balance of the analysis of the pp and np A_y data then is: $g^2_{\pi^0}/4\pi \leq 13.6$ and $g^2_{\pi^\pm}/4\pi \geq 14.0$. Notice that this splitting is consistent with our conclusions in Sect. 2. Thus, we have now some indications for charge-splitting of g_π from two very different observables, namely the deuteron quadrupole moment and np analyzing powers.

Therefore, it is worthwhile to look deeper into the issue of charge-splitting of the πNN coupling constant. Unfortunately, there are severe problems with any substantial charge-splitting—for two reasons. First, theoretical work [20] on isospin symmetry breaking of the πNN coupling constant based upon QCD sum rules comes up with a splitting of less than 0.5% for g^2_π and, thus, cannot explain the large charge splitting indicated above. Second, a problem

occurs with the conventional explanation of the charge-dependence of the singlet scattering length, which we will discuss in the next section.

4 Charge-dependence of the singlet scattering length and charge-dependence of the pion coupling constant

The ultimate purpose of this Section is to show in detail how charge-splitting of the πNN coupling constant affects the charge-dependence of the ${}^1S_0$ scattering length. It will turn out that the charge-splitting of g_π suggested in Sect. 2 and 3 causes a disaster for our established understanding of the charge-dependence of the singlet sattering length.

To set the stage properly, I will first summarize the established empirical and theoretical facts about the charge-dependence of the nuclear force.

The equality between proton-proton (pp) [or neutron-neutron (nn)] and neutron-proton (np) nuclear interactions is known as charge independence—a symmetry that is slightly broken. This is seen most clearly in the ${}^1S_0$ nucleon-nucleon scattering lengths. The latest empirical values for the singlet scattering length a and effective range r are [21, 22]:

$$\begin{array}{ll} a_{pp}^N = -17.3 \pm 0.4 \text{ fm}, & r_{pp}^N = 2.85 \pm 0.04 \text{ fm}, \\ a_{nn}^N = -18.8 \pm 0.3 \text{ fm}, & r_{nn}^N = 2.75 \pm 0.11 \text{ fm}, \\ a_{np} = -23.75 \pm 0.01 \text{ fm}, & r_{np} = 2.75 \pm 0.05 \text{ fm}. \end{array} \quad (1)$$

The values given for pp and nn scattering refer to the nuclear part of the interaction as indicated by the superscript N. Electromagnetic effects have been removed from the experimental values, which is model dependent. The uncertainties quoted for a_{pp}^N and r_{pp}^N are due to this model dependence.

It is useful to define the following averages:

$$\bar{a} \equiv \frac{1}{2}(a_{pp}^N + a_{nn}^N) \;=\; -18.05 \pm 0.5 \text{ fm}, \quad (2)$$

$$\bar{r} \equiv \frac{1}{2}(r_{pp}^N + r_{nn}^N) \;=\; 2.80 \pm 0.12 \text{ fm}. \quad (3)$$

By definition, charge-independence breaking (CIB) is the difference between the average of pp and nn, on the one hand, and np on the other:

$$\Delta a_{CIB} \equiv \bar{a} - a_{np} \;=\; 5.7 \pm 0.5 \text{ fm}, \quad (4)$$

$$\Delta r_{CIB} \equiv \bar{r} - r_{np} \;\; = \;\; 0.05 \pm 0.13 \text{ fm}. \tag{5}$$

Thus, the NN singlet scattering length shows a clear signature of CIB in strong interactions.

The current understanding is that the charge dependence of nuclear forces is due to differences in the up and down quark masses and electromagnetic interactions. On a more phenomenological level, major causes of CIB are the mass splittings of isovector mesons (particularly, π and ρ) and irreducible pion-photon exchanges.

It has been known for a long time that the difference between the charged and neutral pion masses in the one-pion-exchange (OPE) potential accounts for about 50% of Δa_{CIB}. Based upon the Bonn meson-exchange model for the NN interaction [23], also multiple pion exchanges have been taken into account. Including these interactions, about 80% of the empirical Δa_{CIB} can be explained [24, 25]. Ericson and Miller [26] obtained a very similar result using the meson-exchange model of Partovi and Lomon [27].

The CIB effect from OPE can be understood as follows. In nonrelativistic approximation [28] and disregarding isospin factors, OPE is given by

$$V_{1\pi}(g_\pi, m_\pi) = -\frac{g_\pi^2}{4M^2} \frac{(\boldsymbol{\sigma}_1 \cdot \mathbf{k})(\boldsymbol{\sigma}_2 \cdot \mathbf{k})}{m_\pi^2 + \mathbf{k}^2} \left(\frac{\Lambda_\pi^2 - m_\pi^2}{\Lambda_\pi^2 + \mathbf{k}^2} \right)^n \tag{6}$$

with M the average nucleon mass, m_π the pion mass, and $\mathbf{k}$ the momentum transfer. The above expression includes a form factor with cutoff mass Λ_π and exponent n.

For $S = 0$ and $T = 1$, where S and T denote the total spin and isospin of the two-nucleon system, respectively, we have

$$V_{1\pi}^{01}(g_\pi, m_\pi) = \frac{g_\pi^2}{m_\pi^2 + \mathbf{k}^2} \frac{\mathbf{k}^2}{4M^2} \left(\frac{\Lambda^2 - m_\pi^2}{\Lambda^2 + \mathbf{k}^2} \right)^n \;\; , \tag{7}$$

where the superscripts 01 refer to ST. In the ${}^1S_0$ state, this potential expression is repulsive. The charge-dependent OPE is then,

$$V_{1\pi}^{01}(pp) = V_{1\pi}^{01}(g_{\pi^0}, m_{\pi^0}) \tag{8}$$

for pp scattering, and

$$V_{1\pi}^{01}(np) = 2V_{1\pi}^{01}(g_{\pi^\pm}, m_{\pi^\pm}) - V_{1\pi}^{01}(g_{\pi^0}, m_{\pi^0}) \tag{9}$$

Table IV. Predictions for Δa_{CIB} as defined in Eq. (4) in units of fm without and with the assumption of charge-dependence of g_π.

	No charge-dependence of g_π		**Charge-dependent g_π:** $g^2_{\pi^0}/4\pi = 13.6$ $g^2_{\pi^\pm}/4\pi = 14.4$
	Ericson & Miller [26]	Li & Machleidt [25]	
1π	3.50	3.24	–1.58
2π	0.88	0.36	–1.94
$\pi\rho, \pi\sigma, \pi\omega$	—	1.04	–0.97
Sum	4.38	4.64	–4.49
Empirical		5.7 ± 0.5	

for np scattering.

If we assume charge-independence of g_π (i. e., $g_{\pi^0} = g_{\pi^\pm}$), then all CIB comes from the charge splitting of the pion mass, which is [29]

$$m_{\pi^0} = 134.976\text{MeV}, \tag{10}$$

$$m_{\pi^\pm} = 139.570\text{MeV}. \tag{11}$$

Since the pion mass appears in the denominator of OPE, the smaller π^0-mass exchanged in pp scattering generates a larger (repulsive) potential in the $^1S_0$ state as compared to np where also the larger $\pi^\pm$-mass is involved. Moreover, the π^0-exchange in np scattering carries a negative sign, which further weakens the np OPE potential. The bottom line is that the pp potential is more repulsive than the np potential. The quantitative effect on Δa_{CIB} is about 3 fm (cf. Table IV).

We now turn to the CIB created by the 2π exchange (TPE) contribution to the NN interaction. There are many diagrams that contribute (see Ref. [25] for a complete overview). For our qualitative discussion here, we pick the largest of all 2π diagrams, namely, the box diagrams with $N\Delta$ intermediate states, Fig. 4. Disregarding isospin factors and using some drastic approximations [28], the amplitude for such a diagram is

$$V_{2\pi}(g_\pi, m_\pi) = -\frac{g_\pi^4}{16M^4}\frac{72}{25}\int \frac{d^3p}{(2\pi)^3}\frac{[\boldsymbol{\sigma}\cdot\mathbf{k}\boldsymbol{S}\cdot\mathbf{k}]^2}{(m_\pi^2+\mathbf{k}^2)^2(E_p+E_p^\Delta-2E_q)}\left(\frac{\Lambda^2-m_\pi^2}{\Lambda^2+\mathbf{k}^2}\right)^{2n}, \tag{12}$$

where $\mathbf{k} = \mathbf{p} - \mathbf{q}$ with $\mathbf{q}$ the relative momentum in the initial and final state (for simplicity, we are considering a diagonal matrix element); $E_p =$

$\sqrt{M^2+\mathbf{p}^2}$ and $E_p^\Delta = \sqrt{M_\Delta^2+\mathbf{p}^2}$ with $M_\Delta = 1232$ MeV the Δ-isobar mass; $\mathbf{S}$ is the spin transition operator between nucleon and Δ. For the $\pi N\Delta$ coupling constant, $f_{\pi N\Delta}$, the quark-model relationship $f^2_{\pi N\Delta} = \frac{72}{25} f^2_{\pi NN}$ is used [23].

For small momentum transfers $\mathbf{k}$, this attractive contribution is roughly proportional to m_π^{-4}. Thus for TPE, the heavier pions will provide less attraction than the lighter ones. Charged and neutral pion exchanges occur for pp as well as for np, and it is important to take the isospin factors carried by the various diagrams into account. They are given in Fig. 4 below each diagram. For pp scattering, the diagram with double $\pi^\pm$ exchange carries the largest factor, while double $\pi^\pm$ exchange carries only a small relative weight in np scattering. Consequently, pp scattering is less attractive than np scattering which leads to an increase of Δa_{CIB} by 0.79 fm due to the diagrams of Fig. 4. The crossed diagrams of this type reduce this result and including all 2π exchange diagrams one finds a total effect of 0.36 fm [25]. Diagrams that go beyond 2π have also been investigated and contribute another 1 fm. In this way, pion-mass splitting explains about 80% of Δa_{CIB} (see Table IV for a summary).

Recall that our considerations in Sect. 2 sugested charge-splitting of g_π, like

$$g^2_{\pi^0}/4\pi = 13.6\,, \tag{13}$$
$$g^2_{\pi^\pm}/4\pi = 14.4\,, \tag{14}$$

cf. Model E of Table I. We will now discuss how this charge-splitting of g_π affects Δa_{CIB} (more details can be found in the original paper Ref. [30]).

Accidentally, this splitting is—in relative terms—about the same as the pion-mass splitting; that is

$$\frac{g_{\pi^0}}{m_{\pi^0}} \approx \frac{g_{\pi^\pm}}{m_{\pi^\pm}}\,. \tag{15}$$

As discussed, for zero momentum transfer, we habe roughly

$$\mathrm{OPE} \sim \left(\frac{g_\pi}{m_\pi}\right)^2 \tag{16}$$

and

$$\mathrm{TPE} \sim \left(\frac{g_\pi}{m_\pi}\right)^4\,, \tag{17}$$

which is not unexpected, anyhow. On the level of this qualitative discussion, we can then predict that any pionic charge-splitting satisfying Eq. (15) will create no CIB from pion exchanges. Consequently, a charge-splitting of g_π as given in Eqs. (13) and (14) will wipe out our established explanation of CIB of the NN interaction.

We have also conducted accurate numerical calculations based upon the Bonn meson-exchange model for the NN interaction [23]. The details of these calculations are spelled out in Ref. [25] where, however, no charge-splitting of g_π was considered. Assuming the g_π of Eqs. (13) and (14), we obtain the Δa_{CIB} predictions given in the last column of Table IV. It is seen that the results of an accurate calculation go even beyond what the qualitative estimate suggested: the conventional CIB prediction is not only reduced, it is reversed. This is easily understood if one recalls that the pion mass appears in the propagator $(m_\pi^2+\mathbf{k}^2)^{-1}$. Assuming an average $\mathbf{k}^2 \approx m_\pi^2$, the 7% charge splitting of m_π^2 will lead to only about a 3% charge-dependent effect from the propagator. Thus, if a 6% charge-splitting of g_π^2 is used, this will not only override the pion-mass effect, it will reverse it.

Based upon this argument and on our numerical results, one can then estimate that a charge-splitting of g_π^2 of only about 3% (e. g., $g_{\pi^0}^2/4\pi = 13.6$ and $g_{\pi^\pm}^2/4\pi = 14.0$) would erase all CIB prediction of the singlet scattering length derived from pion mass splitting.

Besides pion mass splitting, we do not know of any other essential mechanism to explain the charge-dependence of the singlet scattering length. Therefore, it is unlikely that this mechnism is annihilated by a charge-splitting of g_π. This may be taken as an indication that there is no significant charge splitting of the πNN coupling constant.

5 Conclusions

Several NN observables can be identified that are very sensitive to the πNN coupling constant, g_π. They all carry the potential to determine g_π with high precision.

In particular, we have shown that the pp A_y data below 17 MeV are very sensitive to g_π and imply a value $g_\pi^2/4\pi \approx 13.2$. The np A_y data below 17 MeV show moderate sensitivity and the deuteron quadrupole moment shows great sensitivity to g_π; both np observables imply $g_\pi^2/4\pi \geq 14.0$.

The two different values may suggest a relatively large charge-splitting of g_π. However, in Sect. 4, we have show that a charge-splitting of this kind would completely erase our established explanation of the charge-dependence of the singlet scattering length. Since this is unlikely to be true, we must discard the possibility of any substantial charge-splitting of g_π.

The conclusion then is that we are faced with real and substantial discrepancies between the values for g_π based upon different NN observables. The reason for this can only be that there are large, unknown systematic errors in the data and/or large uncertainties in the theoretical methods. Our homework for the future is to find these errors and eliminate them.

Another way to summarize the current cumbersome situation is to state that, presently, any value between 13.2 and 14.4 is possible for $g_\pi^2/4\pi$ depending on which NN observable you pick. If we want to pin down the value more tightly, then we are faced with three possible scenarios:

- g_π is small, $g_\pi^2/4\pi \leq 13.6$:
  The deuteron η and pp scattering at low energies are described well; there are moderate problems with the np A_y data below 17 MeV. *The most serious problem is the deuteron Q.* Meson-exchange current contributions (MEC) and relativistic corrections for Q of 0.016 fm^2 or more would solve the problem. Present calculations predict about 0.010 fm^2 or less. A serious reinvestigation of this issue is called for. We note that an alternative solution of the problem with Q is to introduce a heavy pion, $\pi'(1200)$. This possibility is discussed in Ref. [5].

- g_π is large, $g_\pi^2/4\pi \geq 14.0$:
  The deuteron Q is well reproduced, but η is predicted too large as compared to the most recent measurement by Rodning and Knutsen [9], $\eta = 0.0256(4)$. Note, however, that all earlier measurements of η came up with a larger value; for example, Borbely *et al.* [31] obtained $\eta = 0.0273(5)$. There are no objectively verifiable reasons why the latter value should be less reliable than the former one. The deuteron η carries the potential of being the best observable to determine g_π (as pointed out repeatedly by Ericson [2] in the 1980's); but the unsettled experimental situation spoils it all. The np A_y data at low energy are described well. *The most serious problem are the pp A_y data below 100 MeV.*

- g_π is 'in the middle', $13.6 \leq g_\pi^2/4\pi \leq 14.0$:
  we have all of the above problems, but in moderate form.

Acknowledgement
This work was supported in part by the U.S. National Science Foundation under Grant No. PHY-9603097.

References

[1] D. V. Bugg and R. Machleidt, Phys. Rev. C **52**, 1203 (1995).

[2] T. E. O. Ericson and M. Rosa-Clot, Nucl. Phys. **A405**, 497 (1983); T. E. O. Ericson, Comments Nucl. Part. Phys. **13**, 157 (1984); T. E. O. Ericson and M. Rosa-Clot, Ann. Rev. Nucl. Part. Sci. **35**, 271 (1985); T. E. O. Ericson and W. Weise, *Pions and Nuclei* (Clarendon Press, Oxford, 1988).

[3] R. Machleidt, F. Sammarruca, and Y. Song, Phys. Rev. C **53**, 1483 (1996).

[4] R. Machleidt and F. Sammarruca, Phys. Rev. Lett. **66**, 564 (1991).

[5] R. Machleidt and G. Q. Li, πN Newsletter **9**, 37 (1993).

[6] From the experimental value for Q, which is 0.2859(3) fm^2 [7, 2], we have subtracted 0.010(2) fm^2 to eliminate contributions obtained from meson-exchange currents and relativistic corrections as calculated by Henning using the Bonn potential [8]. Note that our predictions for Q do not include the latter contributions.

[7] R. V. Reid and M. L. Vaida, Phys. Rev. Lett. **34**, 1064 (1975); D. M. Bishop and L. M. Cheung, Phys. Rev. A **20**, 381 (1979).

[8] H. Henning, privat communication.

[9] N. L. Rodning and L. D. Knutsen, Phys. Rev. C **41**, 898 (1990).

[10] V. G. J. Stoks, R. A. M. Klomp, M. C. M. Rentmeester, and J. J. de Swart, Phys. Rev. C **48**, 792 (1993).

[11] G. Höhler and E. Pietarinen, Nucl. Phys. **B95**, 210 (1975).

[12] J. J. Sakurai, *Currents and Mesons* (University of Chicago Press, Chicago, 1969).

[13] G. E. Brown and R. Machleidt, Phys. Rev. C **50**, 1731 (1994).

[14] SAID, Scattering Analysis Interactive Dial-in facility developed by R. A. Arndt *et al.*, Virginia Polytechnic Institute and State University, The George Washington University, and Jefferson Lab.

[15] Note that in *pp* scattering only the π^0 is exchanged.

[16] J. L. Gammel and R. M. Thaler, Phys. Rev. **107**, 291, 1339 (1957).

[17] M. D. Barker *et al.*, Phys. Rev. Lett. **48**, 918 (1982), *ibid.* **49**, 1056 (1982).

[18] G. J. Weisel *et al.*, Phys. Rev. C **46**, 1599 (1992).

[19] K. Wilczynski *et al.*, Nucl. Phys. **A425**, 458 (1984).

[20] W-Y. P. Hwang *et al.*, Phys. Rev. C **57**, 61 (1998).

[21] G. A. Miller, B. M. K. Nefkens, and I. Slaus, Phys. Reports **194**, 1 (1990).

[22] G. A. Miller and W. H. T. van Oers, In *Symmetries and Fundamental Interactions in Nuclei*, W. C. Haxton and E. M. Henley, eds. (World Scientific, Singapore, 1995) p. 127.

[23] R. Machleidt, K. Holinde, and Ch. Elster, Phys. Reports **149**, 1 (1987).

[24] C. Y. Cheung and R. Machleidt, Phys. Rev. C **34** 1181 (1986).

[25] G. Q. Li and R. Machleidt, Phys. Rev. C **58**, 3153 (1998).

[26] T. E. O. Ericson and G. A. Miller, Phys. Lett. **132B**, 32 (1983).

[27] M. H. Partovi and E. L. Lomon, Phys. Rev. D **2**, 1999 (1970).

[28] For pedagogical reasons, we use simple, approximate expressions when discussing the effects from pion exchange in a qualitative manner. Note, however, that in our numerical calculations we use relativistic time-ordered perturbation theory in its full complexity and without approximations, as outlined in all detail in the appendices of Ref. [23].

[29] Particle Data Group, Phys. Rev. D **54**, 1 (1996).

[30] R. Machleidt and M. K. Banerjee, submitted to Few-Body Systems, nucl-th/9908066.

[31] I. Borbely, W. Grüebler, B. Vuaridel, and V. König, Nucl. Phys. **A503**, 349 (1989).

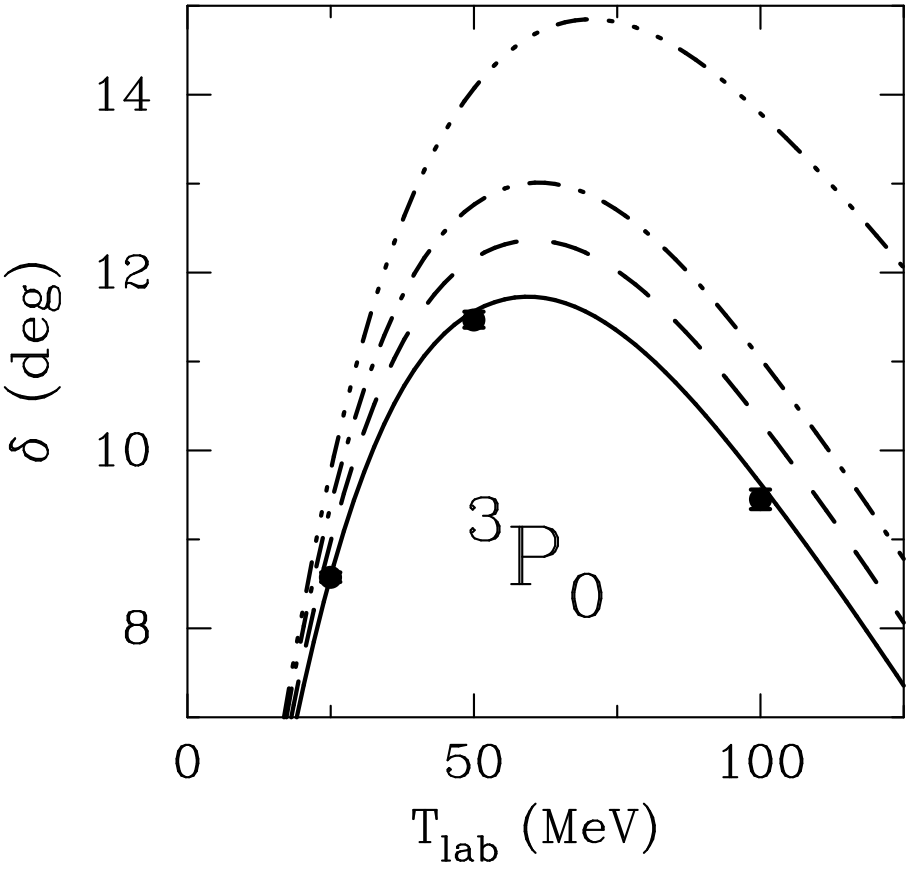

Figure 1: ${}^3P_0$ phase shifts of proton-proton scattering as predicted by Model A and E ($g^2_{\pi^0}/4\pi = 13.6$, solid line), B ($\kappa_\rho = 3.7$, dash-3dot), C ($g^2_{\pi^0}/4\pi = 14.0$, dashed), and D ($g^2_{\pi^0}/4\pi = 14.4$, dash-dot) [15]. The solid dots represent the Nijmegen *pp* multi-energy phase shift analysis [10].

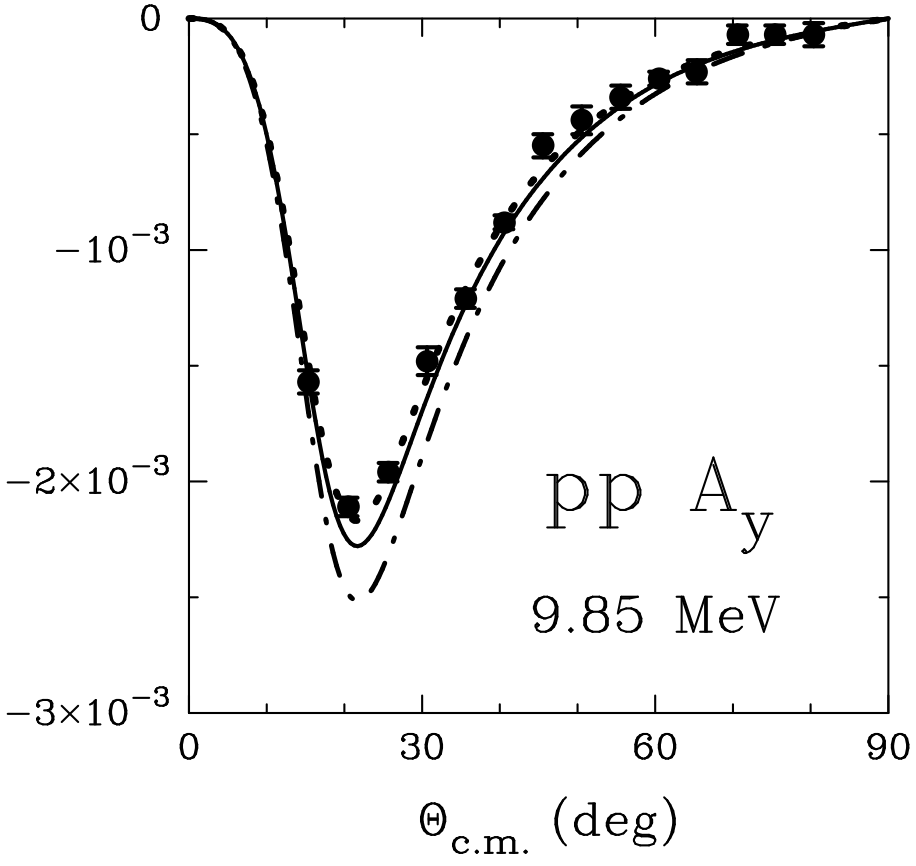

Figure 2: The proton-proton analyzing power A_y at 9.85 MeV. The theoretical curves are calculated with $g^2_{\pi^0}/4\pi = 13.2$ (dotted), 13.6 (solid, Model A), and 14.4 (dash-dot, Model D) and fit the data with a χ^2/datum of 0.98, 2.02, and 9.05, respectively. The solid dots represent the data taken at Wisconsin [17].

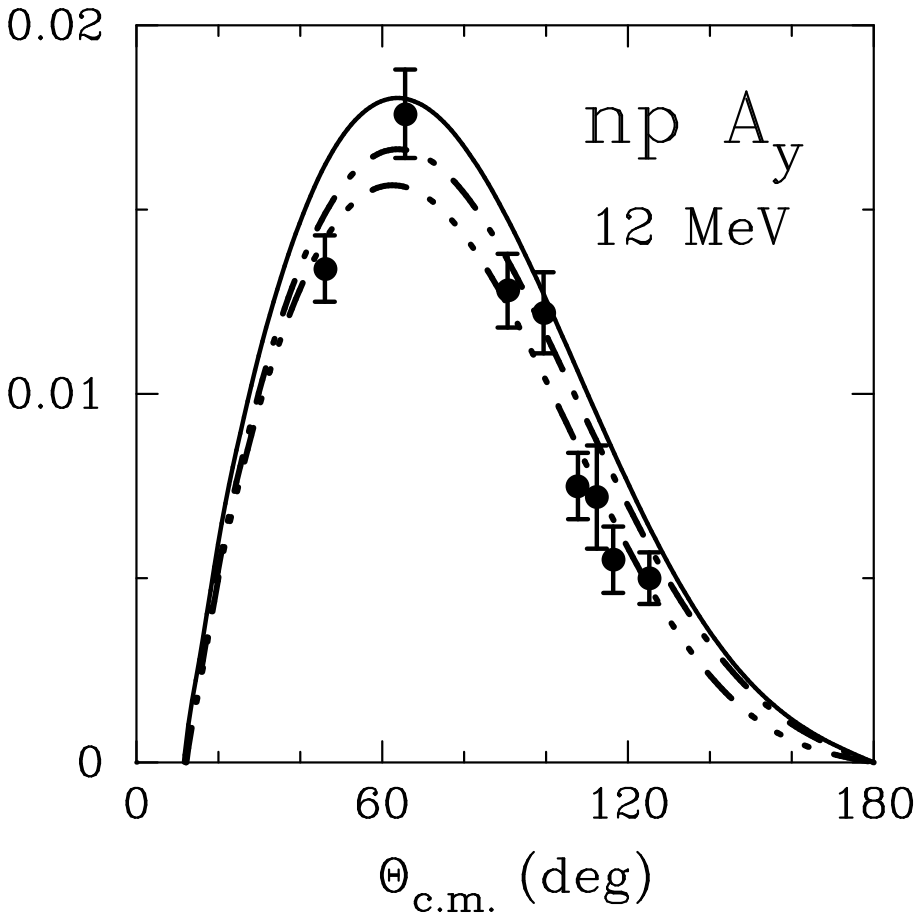

Figure 3: The neutron-proton analyzing power A_y at 12 MeV. The theoretical curves are calculated with $g^2_{\pi^0}/4\pi = g^2_{\pi^\pm}/4\pi = 13.6$ (solid line, Model A), $g^2_{\pi^0}/4\pi = g^2_{\pi^\pm}/4\pi = 14.4$ (dash-dot, Model D), and the charge-splitting $g^2_{\pi^0}/4\pi = 13.6$, $g^2_{\pi^\pm}/4\pi = 14.4$ (dash-3dot, Model E). The solid dots represent the data taken at TUNL [18].

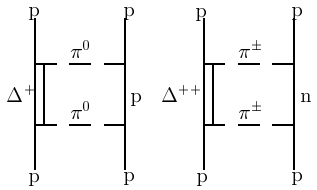

(a)

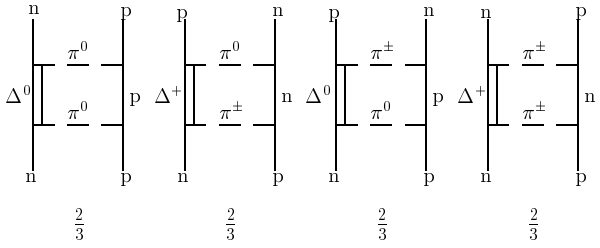

(b)

Figure 4: 2π-exchange box diagrams with $N\Delta$ intermediate states that contribute to (a) *pp* and (b) *np* scattering. The numbers below the diagrams are the isospin factors.

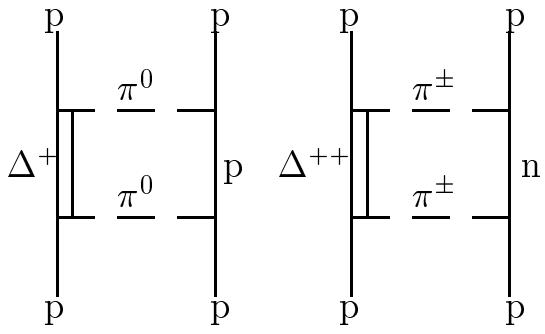

$\frac{2}{3}$ 2

(a)

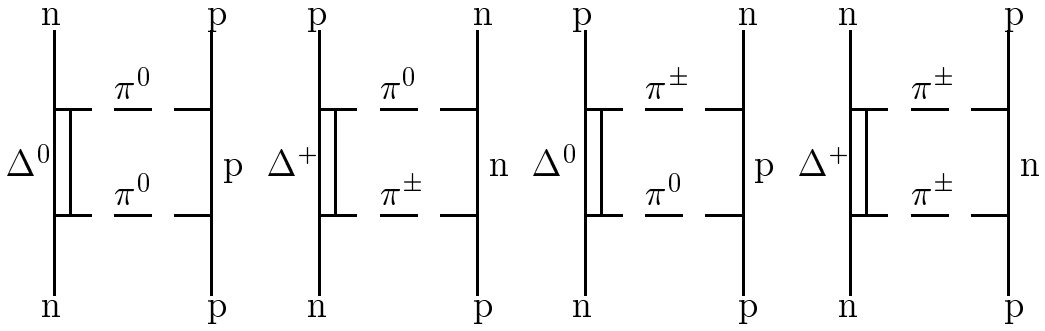

$\frac{2}{3}$ $\frac{2}{3}$ $\frac{2}{3}$ $\frac{2}{3}$

(b)